Mol. Cells *28*, 57-65, July 31, 2009
DOI/10.1007/s10059-009-0101-4

Molecules and Cells

Suppression of the ER-Localized AAA ATPase NgCDC48 Inhibits Tobacco Growth and Development

Hansol Bae, Soo Min Choi, Seong Wook Yang[1], Hyun-Sook Pai, and Woo Taek Kim*

CDC48 is a member of the AAA ATPase superfamily. Yeast CDC48 and its mammalian homolog p97 are implicated in diverse cellular processes, including mitosis, membrane fusion, and ubiquitin-dependent protein degradation. However, the cellular functions of plant CDC48 proteins are largely unknown. In the present study, we performed virus-induced gene silencing (VIGS) screening and found that silencing of a gene encoding a tobacco CDC48 homolog, NgCDC48, resulted in severe abnormalities in leaf and shoot development in tobacco. Furthermore, transgenic tobacco plants (*35S:anti-NgCDC48*), in which the *NgCDC48* gene was suppressed using the antisense RNA method, exhibited severely aberrant development of both vegetative and reproductive organs, resulting in arrested shoot and leaf growth and sterile flowers. Approximately 57-83% of *35S:anti-NgCDC48* plants failed to develop mature organs and died at early stage of development. Scanning electron microscopy showed that both adaxial and abaxial epidermal pavement cells in antisense transgenic leaves were significantly smaller and more numerous than those in wild type leaves. These results indicate that NgCDC48 is critically involved in cell growth and development of tobacco plants. An *in vivo* targeting experiment revealed that NgCDC48 resides in the endoplasmic reticulum (ER) in tobacco protoplasts. We consider the tantalizing possibility that CDC48-mediated degradation of an as-yet unidentified protein(s) in the ER might be a critical step for cell growth and expansion in tobacco leaves.

INTRODUCTION

Cell Division Cycle 48 (CDC48) is a member of the ATPase associated with a variety of cellular activities (AAA) superfamily. Yeast CDC48 and its mammalian homolog p97 are typified by the presence of one or two conserved ATPase domains that are also known as AAA cassettes (Beyer, 1997; Neuwald et al., 1999). The ATPase domain is comprised of Walker A and Walker B motifs, which are involved in ATP binding and hydrolysis, respectively (Beyer, 1997; Neuwald et al., 1999). In yeast and animal systems, CDC48 homologs participate in a wide range of cellular processes, such as mitosis, membrane fusion, and ubiquitin-dependent protein degradation (Decottignies et al., 2003; Fu et al., 2003; Partridge et al., 2003; Richly et al., 2005; Romisch, 2006; Ye et al., 2001; 2003). For example, CDC48 plays a role in nuclear envelope formation and ER and Golgi membrane assembly (Hetzer et al., 2001; Yuan et al., 2001). The CDC48-Ufd1-Npl4 complex functions in ER-associated ubiquitin/26S proteasome-dependent degradation of HMG-CoA reductase, and processing of transcription factor Spt23 (Bays and Hampton, 2002; Jentsch and Rumpf, 2007). CDC48 has been shown to be involved in mitotic spindle dynamics and spindle pole organization (Cao and Zheng, 2004; Cheeseman and Desai, 2004).

Compared to the extensive studies of CDC48 homologs in yeasts and mammals, our understanding of CDC48 in higher plants is rudimentary. In *Arabidopsis*, there are three homologous *AtCDC48* genes encoding AtCDC48A, AtCDC48D, and AtCDC48E, respectively. The *AtCDC48A* gene was isolated and its mRNA was found to be expressed at high levels in proliferating and rapidly expanding cells, but at reduced levels in differentiated cells, suggesting that AtCDC48A may function in cell division and growth in *Arabidopsis* (Feiler et al., 1995). By immunological analysis, the AtCDC48 protein was localized to the plane of cell division during cytokinesis, and implicated in plant cell division processes (Rancour et al., 2002). A more detailed function of AtCDC48A was revealed by loss-of-function T-DNA knockout mutant analysis. Homozygous *atcdc48a* mutant lines exhibited pleiotropic phenotypes, including arrest of seedling development, reduced cell expansion, and defects in pollen and embryo development (Park et al., 2008). In addition, transgenic *Arabidopsis* plants that overexpressed the *AtCDC48A* Walker A mutant form displayed cytokinesis and cell division anomalies and aberrant root hair formation. Thus, these loss-of-function and dominant negative mutant studies indicate multiple roles of AtCDC48 in cell division, growth, and development in *Arabidopsis* (Park et al., 2008).

Department of Biology, College of Life Science and Biotechnology, Yonsei University, Seoul 120-749, Korea, [1]Present address: Host-Pathogen Interaction Group, Temasek Life Sciences Laboratory, National University of Singapore, 117604, Singapore
*Correspondence: wtkim@yonsei.ac.kr

Received May 11, 2009; revised May 29, 2009; accepted June 3, 2009; published online July 8, 2009

Keywords: AAA ATPase CDC48 homolog, antisense suppression, growth and development, tobacco (*Nicotiana tabacum*), virus-induced gene silencing

In the present study, we conducted virus-induced gene silencing (VIGS) screening and found that silencing of cDNA encoding a tobacco CDC48 homolog, NgCDC48, resulted in severe abnormalities in leaf and shoot development in tobacco. Furthermore, we constructed transgenic tobacco plants (*35S:anti-NgCDC48*), in which the *NgCDC48* gene was suppressed using the antisense RNA method. These *35S:an-tisense-NgCDC48* transgenic lines exhibited severely aberrant development in both vegetative and reproductive organs, resulting in arrested shoot and leaf growth and sterile flowers. The results of an *in vivo* targeting experiment indicate that NgCDC48 resides in the endoplasmic reticulum (ER) in tobacco protoplasts. These results are discussed in light of the suggestion that NgCDC48 is critically involved in normal growth and development of tobacco plants. We consider the tantalizing possibility that CDC48-mediated degradation of an as-yet unidentified protein(s) in the ER is a critical step for cell growth and expansion in tobacco leaves.

MATERIALS AND METHODS

Plant materials

Wild type tobacco plants (*Nicotiana benthamiana*, *Nicotiana glutinosa*, and *Nicotiana tabacum*) were grown on 0.8% agar for 4 d in a dark room or on MS medium containing 3% sucrose, vitamin B5 (12 mg L^{-1}), and 0.8% agar (pH 5.8) for 7 d in a growth chamber under a 16-h-light/8-h-dark photoperiod at 25°C (Cho et al., 2008b).

VIGS

The partial *NgCDC48* cDNA fragments were amplified by PCR. PCR-amplified cDNA was then inserted into the pTC00 vector, which contains a part of the TRV genome (Ratcliff et al., 2001), using *Bam*H1 and *Xcm*I sites. VIGS was conducted essentially as described by Park et al. (2005b) with *Nicotiana benthamiana* tobacco plants. The fourth and fifth leaves above the infiltrated leaf were used for RT-PCR and phenotypic analysis (Cho et al., 2008a).

Isolation of a full-length *NgCDC48* cDNA clone

The lambda uni-Zap II tobacco (*Nicotiana glutinosa*) leaf cDNA library was screened using the partial cDNA clone identified from VIGS screening as a probe by an established procedure as described previously (Park et al., 2003). The cDNA inserts containing putative *NgCDC48* were subcloned into the Bluescript SK plasmid by *in vivo* excision of pBluescript from the Zap II vector, as described in Stratagene protocols.

Construction of *35S:anti-NgCDC48* transgenic tobacco plants

The full-length pNgCDC48 cDNA was prepared by PCR using Ex-Taq polymerase (Takara, Japan). The DNA sequences for the primers used were 5′-GGATCCGATGAGTCACCAGGCCGA-3′ and 5′-GGATCCTTAGCTATACAAGTCATCATCATCAG-3′. To facilitate subcloning of PCR products, forward and reverse primers were tagged with cleavage sites for the restriction enzyme *Bam*H1. The tagged cDNA was cloned into the corresponding sites of a binary vector, pCambia1390, in the antisense orientation. The constructed fusion gene product was transferred to *Agrobacterium tumefaciens* strain AGL1 by electroporation, and leaf discs of *Nicotiana tabacum* cv. Samsun NN were transformed by *Agrobacterium*-mediated co-cultivation methods according to Lee et al. (2003). Transgenic tobacco plants were generated on medium containing 40 mg L^{-1} hygromycin B. The regenerated plants were grown in a growth room typically 25°C during the day and 20°C at night. The light/dark cycle in the growth room was 16/8 h. Primary transformants were self-fertilized and seeds were collected. T1 transgenic plants were used for phenotypic analysis.

RNA isolation and RT-PCR

Total RNAs of tobacco leaves were obtained by a method adapted from established protocols with modification as described by Hong et al. (2008). The total RNAs were precipitated overnight at 4°C by the addition of 0.3 vol. 10 M LiCl and precipitated in ethanol. To examine gene expression levels, total leaf RNAs (2 μg) were reverse-transcribed and the cDNAs were amplified with *NgCDC48*-specific primers using Ex-Tag polymerase (Takara) as described previously (Lee et al., 2007). The DNA sequences for gene-specific primers were as follows: NgCDC48M, 5′-AATGGATGTCATTGATCTTGAAG-3′ and 5′-GTGACATACCAAACTTCTCGAAC-3′, NgCDC48C, 5′-GAAGCGAGAATCCTGATTCTATG-3′ and 5′-GTCATCATCATCAGCTCCAGCATT-3′. Amplification of actin (*NgActin*) was carried out using the following primers: 5′-GGATTTGCTGGTGATGATGCT-3′ and 5′-GTGAATTCCAGCAGCTTCCAT-3′.

Measurement of chlorophyll, xanthophyll, and carotenoid contents in tobacco leaves

Leaves from 4-week-old light-grown wild type and *35S:anti-NgCDC48* transgenic tobacco plants were pulverized with liquid nitrogen using Retsch MM301 mixer mill homogenizer. Total pigments were extracted using 80% acetone. The leaf extract was centrifuged 12,000 × *g* for 10 min at 4°C, and the supernatant was analyzed using a spectrophotometer (Beckman model DU800) to measure chlorophyll a (at 663 nm), chlorophyll b (at 646 nm), and xanthophyll + carotenoid (at 470 nm) as described previously (Deng et al., 1991).

Scanning electron microscopy

Scanning electron microscopy was performed as described by Seo et al. (2008) with slight modification. Briefly, leaves collected from wild type and *35S:anti-NgDCD48* transgenic tobacco plants were fixed in FAA solution under a vacuum and dehydrated with a graded ethanol series. The specimens were then critical-point dried in liquid CO_2. The dried samples were mounted and coated with platinum-palladium in a sputter-coater and subjected to scanning electron microscopy (model JSM-6700F; JEOL).

In vivo localization of NgCDC48

The full-length *NgCDC48* cDNA containing the entire coding region was amplified by PCR using Ex Taq polymerase (Takara) and cloned into the soluble-modified green fluorescent protein (GFP) plasmid to generate *35S:GFP-NgCDC48* under the control of the cauliflower mosaic virus (CaMV) 35S promoter. For transient expression, the constructed plasmid was introduced into protoplasts prepared from tobacco leaves by polyethylene glycol (PEG)-mediated transformation as described by Cho et al. (2008b). After 16 h of incubation, the protoplasts were viewed with a cooled CCD camera and a BX51 fluorescence microscope (Olympus, Japan) as described previously (Lee et al., 2009). To confirm the ER-localized staining pattern, ER-Tracker Blue-White DPX (Invitrogen, USA) was used to stain the protoplasts as a marker for ER localization, and the blue fluorescent signal from this dye was detected with a long-pass DAPI filter. Tobacco telomere repeat binding factor 1, NgTRF1, was used as a marker for nuclear localization (Yang et al., 2003; 2004).

RESULTS

Isolation and characterization of *NgCDC48* cDNA in tobacco plants

We previously conducted VIGS screening using randomly selected cDNAs prepared from mRNAs of various tissues of tobacco plants (Park et al., 2005a; 2005b). The average length of cDNAs used for VIGS screening was approximately 800-900 bp (Kim et al., 2006; Sarowar et al., 2008). We found that silencing of cDNA clone No. 34 produced severe abnormalities in leaf and shoot development in tobacco. Subsequent DNA sequencing analysis of this clone revealed that it encodes a putative yeast CDC48 and human p97 homolog. We next proceeded to isolate a full-length cDNA clone. A partial cDNA fragment of clone No. 34 was radioactively labeled and used as a probe to screen a uni-ZAP II cDNA library constructed from mature leaves of tobacco plants. Several cDNA clones encoding a putative tobacco *NgCDC48* (*Nicotiana glutinosa CDC48*) homolog were isolated. The coding region of full-length *NgCDC48* cDNA (GenBank accession number GQ131539) is 2,415 bp long and encodes an 805-amino acid protein with a predicted molecular mass of 89.4 kDa, similar to that of yeast (92.0 kDa), human (89.3 kDa), and *Arabidopsis* (89.4-90.4 kDa) CDC48 proteins (Fig. 1A). As in other CDC48 homologs, the NgCDC48 protein contains two conserved ATPase domains, in which the Walker A and Walker B motifs are well conserved. Multiple alignments of the deduced amino acid sequence of NgCDC48 with those of previously identified CDC48 proteins are shown in Fig. 1B. NgCDC48 is 91-92% and 92% identical to the *Arabidopsis* and rice proteins, respectively. In addition, NgCDC48 shares a significant degree of sequence identity with the yeast (68%) and human (78%) proteins (Figs. 1B and 1C). Overall, this structural conservation indicates that NgCDC48 is a tobacco homolog of *Arabidopsis* AtCDC48 and yeast CDC48.

VIGS and anti-sense suppression of *NgCDC48* resulted in severe developmental defects in tobacco plants

To verify the effect of *NgCDC48* silencing, two different partial *NgCDC48* cDNA fragments were cloned into the TRV-based VIGS vector pTV00 (Ratcliff et al., 2001) and resulting constructs were transformed into *Agrobacterium*. *Agrobacterium* cells containing each VIGS-cDNA fragment were then infiltrated into tobacco plants by the established method (Park et al., 2005a; 2005b). The *TRV:NgCDC48M* construct contained a middle region of the cDNA, and the *TRV:NgCDC48C* construct comprised the C-terminal coding region and a part of the 3′-untranslated region (Fig. 2A). As shown in Figs. 2B and 2C, VIGS with both constructs produced very similar phenotypes of anomalous tobacco development. Shoot apical growth was arrested resulting in short height, and leaves were small and curled with amorphous shapes. Silencing of *NgCDC48* also resulted in retarded formation of floral organs (see Fig. 3). To examine whether the abnormal phenotypes of VIGS tobacco plants were due to the silencing of the *NgCDC48* gene, the level of endogenous *NgCDC48* mRNA was monitored by RT-PCR using two different sets of gene-specific primers. The results in Fig. 2D show that the amount of *NgCDC48* mRNA was markedly reduced in both *TRV:NgCDC48M* and *TRV:NgCDC48C* lines compared to the TRV control plant, confirming that the expression of the *NgCDC48* gene was effectively suppressed by VIGS.

To corroborate the results of VIGS, we next constructed transgenic tobacco plants, in which expression of *NgCDC48* was suppressed by the antisense RNA method. A CaMV 35S promoter-antisense pNgCDC48 construct (*35S:anti-NgCDC48*) was introduced into tobacco leaf discs using the *Agrobacterium tumefaciens*-mediated transformation method (Lee and Kim, 2003) (Fig. 3A). Independent primary transformed plants were selected by resistance to hygromycin, and numerous T1 transgenic tobacco plants were subsequently obtained. As shown in Fig. 3B, a markedly lower level of *NgCDC48* mRNA was detected in *35S:anti-NgCDC48* transgenic plants relative to that in wild-type tobacco, although actin mRNA level remained unchanged. These antisense lines exhibited severe growth retardation, which is similar to the phenotype of VIGS lines (Fig. 3C). Apical growth of their shoots was impaired and leaf development appeared to be severely defective. The severity of phenotypes was closely associated with the level of endogenous *NgCDC48* transcript. Antisense lines #1 and #4, which showed strong suppression, exhibited severe abnormal growth phenotypes, but line #2, in which the mRNA level was moderately decreased, displayed a mild phenotype (Figs. 3D-3G). This indicates that NgCDC48 plays a critical role in the development of vegetative organs. In addition, as shown in Fig. 3I, development of floral organs in *35S:anti-NgCDC48* plants was critically impaired, and the flowers of these plants were unable to produce viable seeds. Among 14 T1 *35S:anti-NgCDC48* #1 plants investigated, four (28.6%) displayed retarded leaf and shoot growth, two (14.3%) exhibited an albino-like phenotype, and eight (57.1%) displayed lethal phenotypes (Table 1). In the case of *35S:anti-NgCDC48* #4, the percentage of lethal phenotypes was higher, and up to 83.3% (10/12) of the transgenic plants failed to develop mature organs and eventually died (Table 1). Taken together, the results of VIGS and antisense suppression studies support the idea that NgCDC48 participates in the growth and development of both vegetative and reproductive organs in tobacco plants.

Table 1. Frequency (%) of abnormal phenotypes (T1)

Genotype (n)	Retarded growth	Albino-like	Lethal
Wild-type (35)	0.00	0.00	0.00
35S:anti-NgCDC48 #1 (14)	28.6	14.3	57.1
35S:anti-NgCDC48 #4 (12)	16.7	0.00	83.3

Cell expansion rather than cell division is impaired in *35S:anti-NgCDC48* transgenic leaves

The aforementioned results show that NgCDC48 is critically involved in the normal growth and development of tobacco plants, with the suppression of this gene resulting in severely abnormal phenotypes. Based on these results, we considered three possibilities for the cellular function of NgCDC48. The first is that NgCDC48 may participate in the expansion and elongation of the cells. Alternatively, NgCDC48 may be mainly involved in cell division program and, for this reason, silencing of *NgCDC48* may have arrested cell proliferation. Finally, it is possible that NgCDC48 plays a role in both cell expansion and division, as is the case for *Arabidopsis* AtCDC48A (Park et al., 2008). To address these possibilities, we inspected the detailed pattern of leaf development. Figure 4A shows a morphological comparison of leaves from 4-week-old light-grown wild type and *35S:anti-NgCDC48* transgenic tobacco plants. During our search for phenotypic differences, we observed that the morphology of cotyledons and first and second leaves was somewhat similar between wild type and antisense transgenic lines, with the antisense leaves being slightly smaller and more yel-

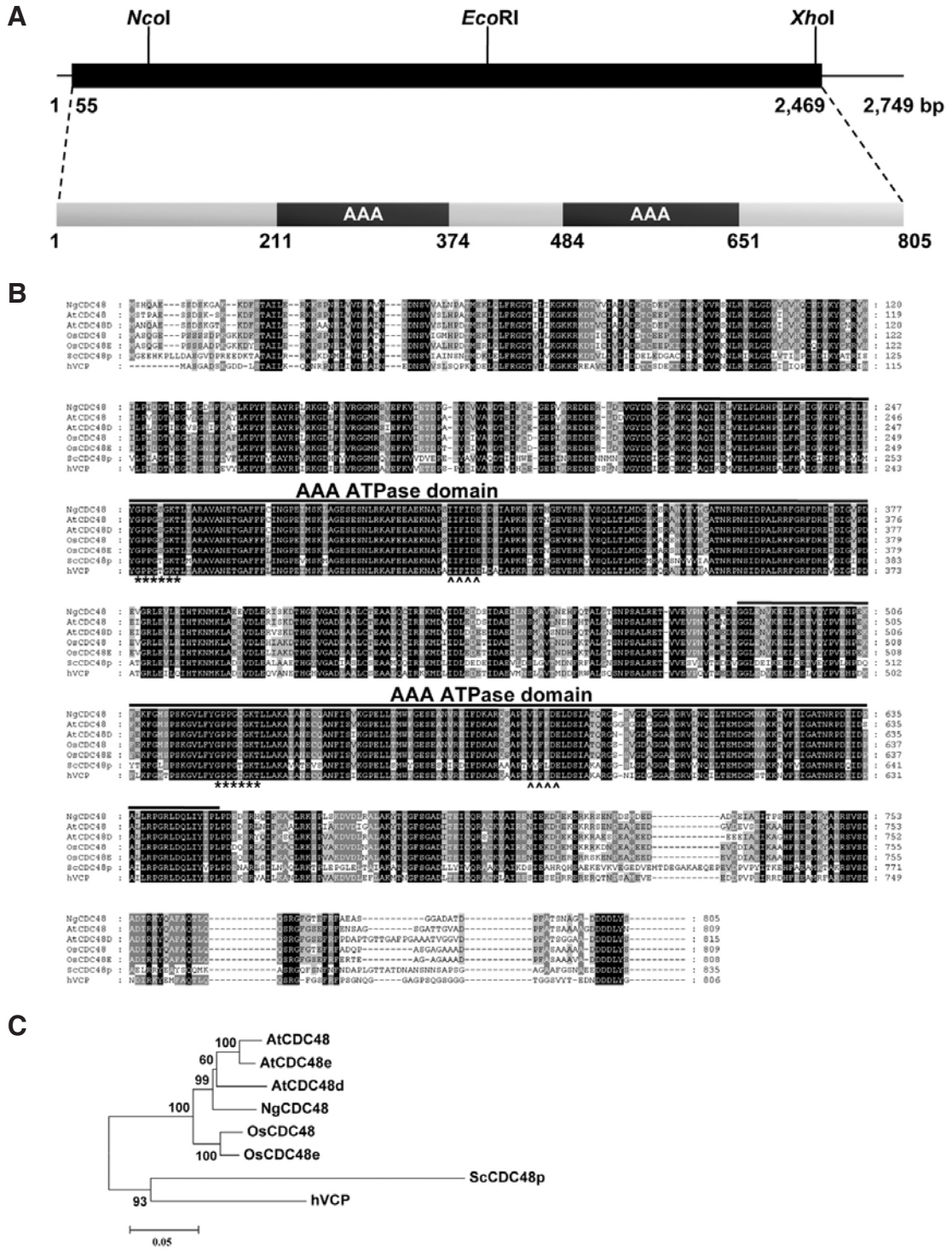

Fig. 1. Sequence analysis of tobacco NgCDC48. (A) Schematic structure of *NgCDC48* cDNA (GenBank accession number GQ131539) and its predicted protein. The solid bar indicates the coding region, and solid lines show 5′- and 3′-untranslated regions. Two AAA ATPase domains are indicated in the predicted protein. (B) Comparison of the deduced amino acid sequence of tobacco NgCDC48 with that of CDC48 homologs from *Arabidopsis* (AtCDC48 and AtCDC48D), rice (OsCDC48 and OsCDC48E), yeast (ScCDC48p), and human (hVCP). Amino acids that are identical in all seven proteins are shown in black. Amino-acid residues that are conserved in at least four of the seven sequences are shaded. The solid lines represent two highly conserved AAA cassette domains. The Walker A and Walker B motifs are indicated by asterisk and arrowheads, respectively. Dashes show gaps introduced into the amino acid sequences for optimal sequence alignment. (C) Phylogenetic analysis of CDC48 proteins from tobacco (NgCDC48), *Arabidopsis* (AtCDC48, AtCDC48D, and AtCDC48E), rice (OsCDC48 and OsCDC48E), yeast (ScCDC48p), and human (hVCP). The dendrogram was constructed using MEGA4 software with the neighbor-joining method. The tree is drawn to scale, with branch lengths representing units of evolutionary distance.

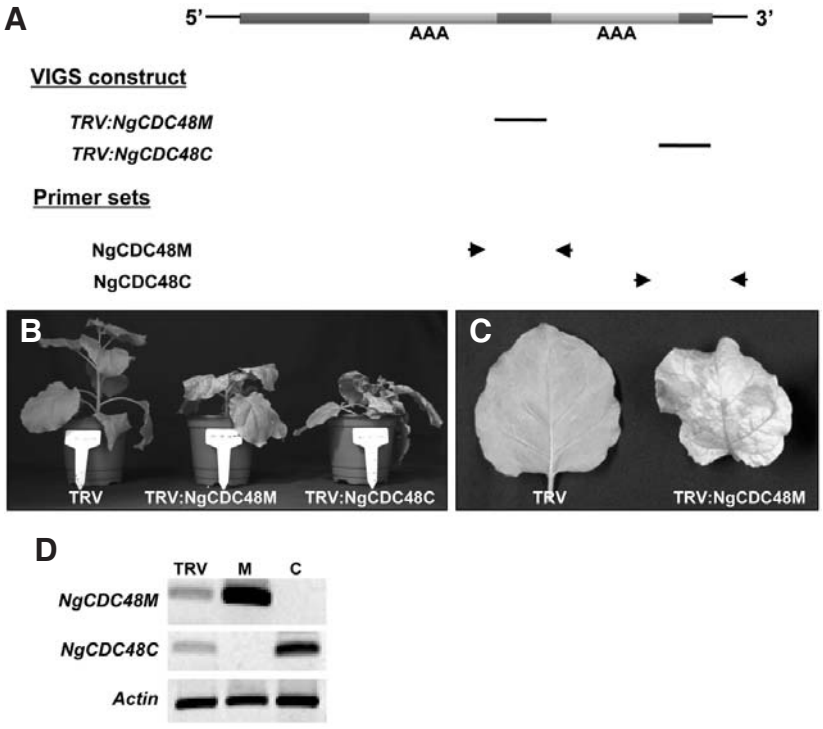

Fig. 2. Silencing of *NgCDC48* by VIGS. (A) Schematic diagram of *NgCDC48* and two different VIGS constructs (*TRV:NgCDC48M* and *TRV:NgCDC48C*) that contain partial fragments of *NgCDC48* cDNA. Regions used for VIGS are indicated by solid lines. The positions of the gene-specific RT-PCR primer sets are shown. (B-C) Growth retardation phenotypes of the *NgCDC48-VIGS* lines. Whole plants and leaves were photographed at 20 days after inoculation. The VIGS leaves were small and curled with amorphous shapes. (D) RT-PCR analysis to investigate the endogenous mRNA levels of *NgCDC48* in TRV control and VIGS plants. Total RNAs were obtained from the leaf tissue of tobacco plants infected by *TRV*, *TRV:NgCDC48M*, and *TRV:NgCDC48C*, respectively. The Ng CDC48M and NgCDC48C primers were used for RT-PCR. The level of actin mRNA was determined as a loading control.

lowish than those of the wild type. In spite of their similar morphology, the fresh weight of the first and second leaves of the antisense transgenic plants was quite different from that of wild type leaves (Fig. 4B, see below). On the other hand, leaf growth was greatly impaired in the third leaves of the antisense plants, so that the morphology as well as the growth pattern of the third leaves was clearly different from those of the wild type plants (Fig. 4A). Moreover, under our experimental conditions, antisense transgenic leaves from the fourth to seventh positions were defective and failed to develop to mature form. These morphological differences were closely associated with the leaf fresh weight as indicated in Figure 4B. The fresh weights of the third, fourth, fifth, and sixth leaves were 0.20 g, 0.28 g, 0.26 g, and 0.11 g, respectively, in wild type tobacco, whereas they were 0.013-0.025 g, 0.015-0.033 g, 0.015-0.028 g, and 0.021-0.024 g, respectively, in antisense transgenic lines #1 and #4 (Fig. 4B). Intriguingly, antisense leaves from the fourth to sixth positions were significantly darker than those of wild type plants (Fig. 4A). These antisense leaves contained 112 $\pm$ 14-160 $\pm$ 24 μg/g. FW of chlorophyll a + chlorophyll b, although wild type leaves had 58 $\pm$ 20-67 $\pm$ 21 μg/g. FW of chlorophyll a + chlorophyll b (Fig. 4C). The amount of xanthophylls and carotenoids was undistinguishable in wild type and antisense lines. Thus, the dark green color of antisense leaves was due to the higher chlorophyll content per fresh weight compared to that of the wild type. This raises the possibility that the smaller leaf size in the antisense transgenic plants may result from reduced cell expansion rather than a decreased rate of cell division.

The more detailed phenotype was further examined by microscopic analysis. We investigated the cellular patterns in the epidermal cell layers of third leaves in 4-week-old wild type and antisense plants using scanning electron microscopy. As indicated in Figs. 5A-5F, both adaxial and abaxial epidermal pavement cells in antisense lines #1 and #4 were significantly smaller and more numerous than those in control plants. Cell number per 10^{-3} cm^2 in adaxial and abaxial epidermis was 26 $\pm$ 4 and 25 $\pm$ 4, respectively, in wild type tobacco, whereas cell number per 10^{-3} cm^2 was markedly increased to 68 $\pm$ 4 and 70 $\pm$ 8 in the epidermal layers of the antisense transgenic plants (Fig. 5G). In contrast, the number of stomata per 100 cells appeared to be similar between wild type and antisense epidermal cell layers (Fig. 5H), indicating that suppression of *NgCDC48* decreased leaf cell size in antisense transgenic plants. Collectively, we interpreted these results as evidence that NgCDC48 is involved in the process of cell expansion during normal growth and development of leaf tissue in tobacco plants.

NgCDC48 is primarily localized to the ER in tobacco protoplasts

To determine the cellular localization of NgCDC48, we performed an *in vivo* targeting experiment employing NgCDC48-fused GFP as a fluorescent marker in a transient transfection assay using protoplasts prepared from wild type mature leaves. The *GFP* gene was fused to the 5′ end of the *NgCDC48* coding region in-frame under the control of the CaMV 35S promoter. The resulting construct was transfected into tobacco leaf protoplasts using PEG (Cho et al., 2008b). Localization of fusion proteins was then determined by visualization with a fluorescence microscope (Lee et al., 2009). As shown in Fig. 6A, the control GFP was uniformly distributed throughout the cytosolic fraction of protoplasts. By contrast, the GFP-NgCDC48 fusion proteins exhibited a network pattern exclusively, suggesting that GFP-NgCDC48 is predominantly localized to the ER (Fig. 6B). To confirm the ER localization, we tested whether the GFP-NgCDC48 fusion protein co-localizes with ER-Tracker Blue-White DPX, an ER marker. The green fluorescent signal of GFP-NgCDC48 closely overlapped with the blue fluorescent signal of ER-Tracker (Fig. 6B). The auto-fluorescent signal of chlorophyll did not co-localize with the ER-specific network signal. We next determined the localization of tobacco double-

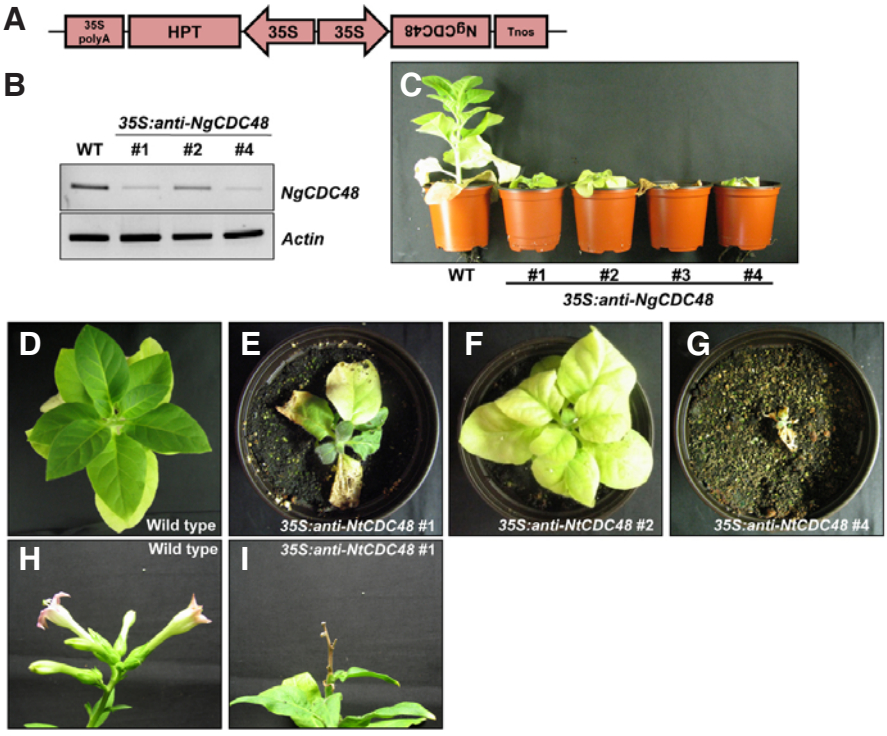

Fig. 3. Vector construct and phenotypic analysis of *35S:anti-NgCDC48* transgenic plants. (A) Schematic representation of the *35S:anti-NgCDC48* binary vector construct for tobacco transformation. (B) Antisense suppression of *NgCDC48* mRNA. Total RNAs were obtained from the leaf tissue of T1 *35S:anti-NgCDC48* transgenic tobacco lines #1, #2, and #4. The level of actin mRNA was used as a loading control. (C-G) Growth retardation phenotypes of 4-week-old light-grown T1 *35S:anti-NgCDC48* transgenic tobacco lines. The *35S:anti-NgCDC48* plants exhibit aberrant growth in leaves and shoots. (H-I) Developmental abnormalities of floral organs in the *35S:anti-NgCDC48* transgenic line. Flowers of *35S:anti-NgCDC48* transgenic tobacco plants were unable to produce viable seeds.

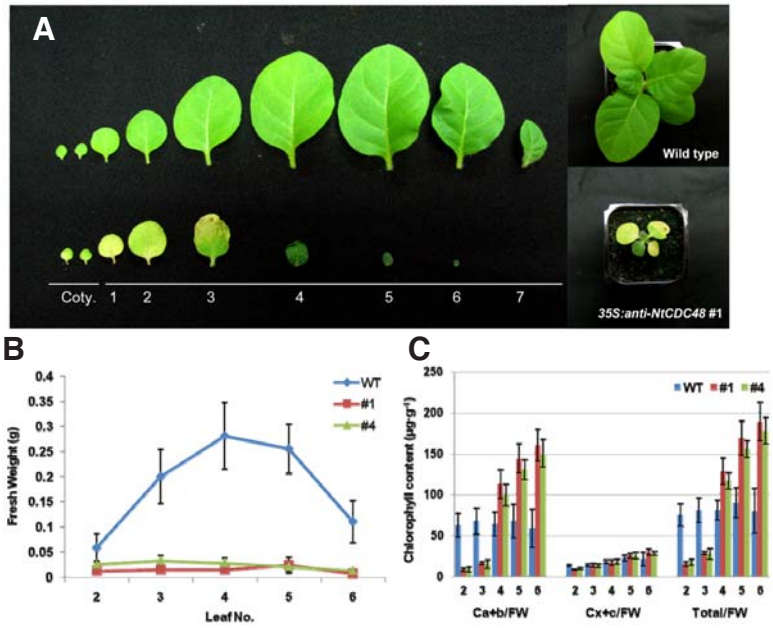

Fig. 4. Morphology, fresh weight, and chlorophyll contents of wild type and *35S:anti-NgCDC48* transgenic leaves (A) Morphological comparison of leaves from 4-week-old light-grown wild type and T1 *35S:anti-NgCDC48* transgenic tobacco plants. (B) Fresh weight of leaves from 4-week-old light-grown wild type and antisense plants. The values are means ± SD (n = 6). (C) Amount of chlorophyll a, chlorophyll b, xanthophyll, and carotenoids in wild type and antisense leaves. Ca+b, the amount of chlorophyll a + chlorophyll b; Cx+c, the amount of xanthophyll + carotenoids; Total, total amount of pigments. The values are means ± SD (n = 6).

strand specific telomere repeat binding factor 1 (NgTRF1) (Yang et al., 2003; 2004) as a nuclear protein control. As previously demonstrated, NgTRF1 was clearly localized in the nuclei (Fig. 6C). On the basis of these *in vivo* targeting results, we conclude that the NgCDC48 protein resides predominantly in the ER in tobacco leaves.

DISCUSSION

VIGS is a gene-inactivation technique based on the phenomenon that expression of a target gene is suppressed in a sequence-specific fashion as a result of infection with a viral vector harboring a part of target gene sequence (Kim et al., 2006; Park et al., 2005a; 2005b; Sarowar et al., 2008). The initial VIGS screening using randomly selected tobacco leaf cDNAs led us to identify a gene that encodes a tobacco NgCDC48 homolog. As is the case for yeast, human, and *Arabidopsis* CDC48 proteins, NgCDC48 contains highly conserved two AAA ATPase domains (Fig. 1). NgCDC48 is remarkably homologous not only to plant proteins (about 90% identity), but

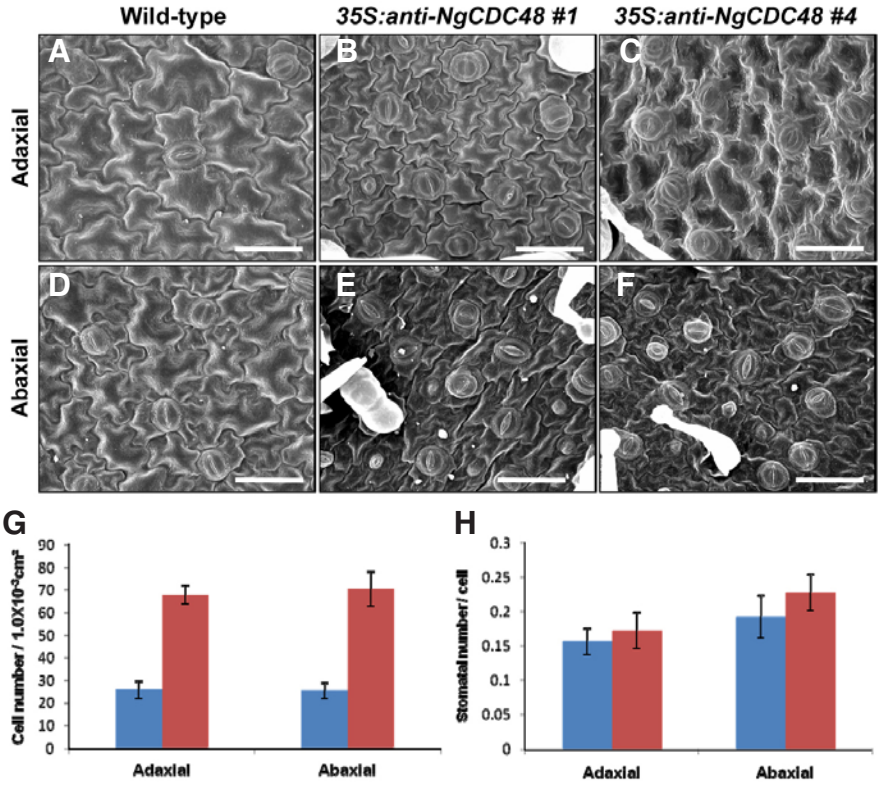

Fig. 5. Scanning electron micrographs and cell number in wild type and *35S:anti-NgCDC48* transgenic leaves. (A-F) Both adaxial and abaxial epidermal pavement cell layers of third leaves in 4-week-old wild type and T1 antisense transgenic (*35S:anti-NgCDC48* #1 and #4) plants were used for scanning electron microscopy. Scale bars, 60 μm. (G) Cell number per 10^{-3} cm^2 in adaxial and abaxial epidermis of wild type and antisense line (*35S:anti-NgCDC48* #1). Blue bars indicate the wild type, and red bars show the antisense transgenic line. The values are means ± SD (n = 3). (H) Stomatal number per 100 cells in adaxial and abaxial epidermis of wild type and antisense line (*35S:anti-NgCDC48* #1). Blue bars indicate the wild type, and red bars show antisense transgenic line. The values are means ± SD (n = 3).

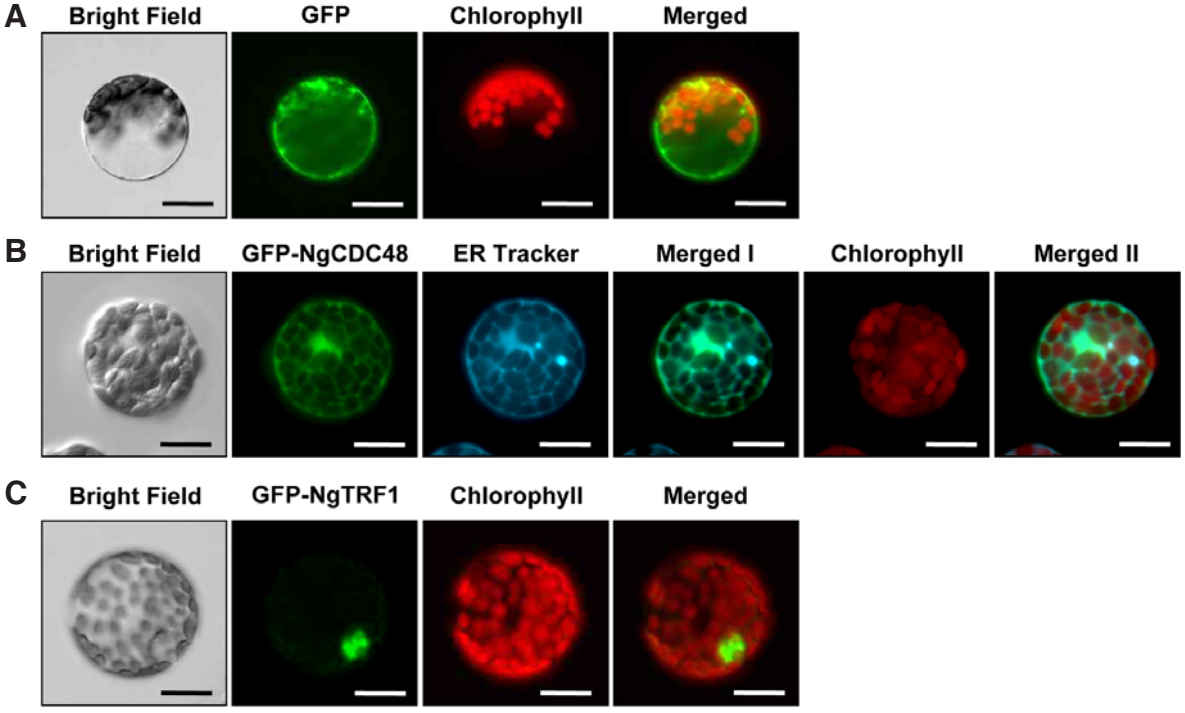

Fig. 6. Cellular localization of NgCDC48 protein. The *35S:GFP* (A), *35S:GFP-NgCDC48* (B), and *35S:GFP-NgTRF1* (C) constructs were transformed into protoplasts obtained from tobacco leaves using the PEG-mediated method. The GFP-fusion proteins were visualized 16 h after transformation using a cooled CCD camera and a fluorescence microscope. The signal for ER-Tracker Blue-White DPX, a photo-stable probe selective for the ER in live cells, shows specific ER localization. The green fluorescent signal of GFP-NgCDC48 closely overlapped with the blue fluorescent signal of ER-Tracker. The red signal shows auto-fluorescence of chloroplasts, which did not overlap with the ER signal. Tobacco telomere-repeat binding factor 1 (NgTRF1), which is localized in the nuclei, is shown as a specificity control. Scale bars, 20 μm.

also to yeast and human proteins (68% and 78%, respectively), suggesting that the mode of action of CDC48 homologs may be conserved in these organisms. However, the cellular roles of plant CDC48 proteins are largely unknown, and most studies of CDC48 in plants have been performed with *Arabidopsis*, a dicot model plant. The AtCDC48A protein was recently implicated in cell division, growth, and development (Park et al., 2008; Rancour et al., 2002). This factor prompted us to explore the possible function of NgCDC48 in tobacco, another dicot model plant.

To confirm the initial gene silencing screening for *NgCDC48*, we repeated the VISG experiment using two different partial *NgCDC48* cDNA fragments and found that the *NgCDC48* silencing resulted in abnormalities in shoot and leaf development (Fig. 2). VIGS, however, produces transient suppression of a target gene (Waterhouse et al., 2001). Thus, to substantiate the results of VIGS, we next constructed transgenic tobacco plants (*35S:anti-NgCDC48*) in which the *NgCDC48* gene was suppressed using the antisense RNA technique (Fig. 3). These *35S:anti-NgCDC48* transgenic lines exhibited severely aberrant development in both vegetative and reproductive organs, resulting in arrested shoot and leaf growth and sterile flowers. The degree of phenotypic severity seems to be closely coupled to the endogenous *NgCDC48* mRNAs in antisense lines and, hence, it is most likely that NgCDC48 is critically involved in normal growth and development in tobacco plants (Figs. 3 and 4). In addition, scanning electron microscopy indicated that NgCDC48 participates in the process of cell elongation and expansion in tobacco leaves (Fig. 5).

Therefore, our VIGS and antisense transgenic approaches support the view that NgCDC48 is essential for the proper formation of vegetative and reproductive organs in tobacco plants. The critical problem that remains to be unraveled is the physiological link between the functional relevance of NgCDC48 and developmental processes in tobacco plants. *Arabidopsis* AtCDC48A forms hexameric complex (Aker et al., 2007) and has been shown to interact with various protein partners, including ubiquitin regulatory X domain-containing protein (PUX1), somatic embryogenesis receptor-like kinase 1 (AtSERK1), and calmodulin-interacting protein (CIP111) (Buaboocha et al., 2001; Park et al., 2007; Rancour et al., 2004; Rienties et al., 2005). In addition, in yeast and mammalian cells, CDC48 plays a role in ubiquitin/26S proteasome-dependent protein degradation in the ER (Bays and Hampton, 2002; Jentsch and Rumpf, 2007; Richly et al., 2005; Romisch, 2006). Our *in vivo* targeting experiment indicates that tobacco NgCDC48 is localized to the ER (Fig. 6). Thus, we are tempted to consider the tantalizing possibility that NgCDC48 is involve in ER-associated degradation of an as-yet unidentified target protein(s), and NgCDC48-mediated protein degradation, in turn, is required for normal growth and development of tobacco plants. We are currently conducting a yeast two-hybrid screen to identify NgCDC48-interacting proteins. Further experiments are required to elucidate the mode of action of NgCDC48 and its interacting proteins in tobacco plant.

ACKNOWLEDGMENTS

This work was supported by grants from the Plant Diversity Research Center (21st Century Frontier Research Program funded by the Ministry of Education, Science, and Technology), the BioGreen 21 Program (funded by the Rural Development Administration), and the Technology Development Program for Agriculture and Forestry (project No. 309017-5 funded by the Ministry for Agriculture, Forestry and Fisheries, Republic of Korea). H.B. was the recipient of a Brain Korea 21 graduate student scholarship.

REFERENCES

Aker, J., Hesselink, R., Engel, R., Karlova, R., Borst J.W., Visser, A.J.W.G., and de Vries, S.C. (2007). *In vivo* hexamerization and characterization of the Arabidopsis AAA ATPase CDC48A complex using Forster resonance energy transfer-fluorescence lifetime imaging microscopy and fluorescence correlation spectroscopy. Plant Physiol. *145*, 339-350.

Bays, N.W., and Hampton, R.Y. (2002). Cdc48-Ufd1-Npl4: Stuck in the middle with Ub, Curr. Biol. *12*, R366-371.

Beyer, A. (1997). Sequence analysis of the AAA protein family. Protein Sci. *6*, 2043-2058.

Buaboocha, T., Liao, B., and Zielinski, R.E. (2001). Isolation of cDNA and genomic DNA clones encoding a calmodulin-binding protein related to a family of ATPases involved in cell division and vesicle fusion. Planta *212*, 774-781.

Cao, K., and Zheng, Y. (2004). The Cdc48/p97-Ufd1-Npl4 complex: its potential role in coordinating cellular morphogenesis during the M-G1 transition. Cell Cycle *3*, 422-424.

Cheeseman, I.M., and Desai, A (2004). Cell division: AAAtacking the mitotic spindle. Curr. Biol. *14*, R70-72.

Cho, H.-K., Park, J.-A., and Pai, H.-S. (2008a). Physiological function of NbRanBP1 in *Nicotiana benthamiana*. Mol. Cells *26*, 270-277.

Cho, S.K, Ryu, M.Y., Song, C., Kwak, J.M., and Kim, W.T. (2008b). *Arabidopsis* PUB22 and PUB23 are homologous U-box E3 ubiquitin ligases that play combinatory roles in response to drought stress. Plant Cell *20*, 1899-1914.

Decottignies, A., Evain, A., and Ghislain, M. (2004). Binding of Cdc48p to a ubiquitin-related UBX domain from novel yeast proteins involved in intracellular proteolysis and sporulation, Yeast *21*, 127-139.

Deng, X.W., Caspar, T., and Quail, P.H. (1991). cop1: a regulatory locus involved in light-controlled development and gene expression in Arabidopsis. Genes Dev. *5*, 1172-1182.

Feiler, H.S., Desprez, T., Santoni, V., Kronenberger, J., Caboche, M., and Traas, J. (1995). The higher plant *Arabidopsis thaliana* encodes a functional *CDC48* homologue which is highly expressed in dividing and expanding cells. EMBO J. *14*, 5626-5637.

Fu, X., Ng, C., Feng, D., and Liang, C. (2003). Cdc48p is required for the cell cycle commitment point at start via degradation of the G1-CDK inhibitor Far1p. J. Cell Biol. *163*, 21-26.

Hetzer, M., Meyer, H.H., Walther, T.C., Biobao-Cortes, D., Warren, G., and Mattaj, I.W. (2001). Distinct AAA-ATPase p97 complexes function in discrete steps of nuclear assembly. Nat. Cell Biol. *3*, 1086-1091.

Hong, J.K., Hwang, J.E., Chung, W.S., Lee, K.O., Choi, Y.J., Gal, S.W., Park, B.-S., and Lim, C.O. (2008). Expression of a chinese cabbage cysteine protease inhibitor, BrCYS1, retards seed germination and plant growth in transgenic tobacco plants. J. Plant Biol. *51*, 347-353.

Jentsch, S., and Rumpf, S. (2007). Cdc48 (p97): a "molecular gearbox" in the ubiquitin pathway? Trends Biochem. Sci. *32*, 6-11.

Kim, M., Lim, J.-H., Ahn, C.S., Park, K., Kim, G.T., Kim, W.T., and Pai, H.-S. (2006). Mitochondria-associated hexokinase play a role in the control of programmed cell death in *Nicotiana benthamiana*. Plant Cell *18*, 2341-2355.

Lee, J.-H., and Kim, W.T. (2003). Molecular and biochemical characterization of *VR-EILs* encoding mung bean ETHYLENE INSENSITIVE3-LIKE proteins. Plant Physiol. *132*, 1475-1488.

Lee, J.-H., Hong, J.-P., Oh, S.-K., Lee, S., Choi, D., and Kim, W.T. (2004). The ethylene-responsive factor like protein 1 (CaERFLP1) of hot pepper (*Capsicum annuum* L.) interacts *in vitro* with both GCC and DRE/CRT sequences with different binding affinities: possible biological roles of CaERFLP1 in response to pathogen infection and high salinity conditions in transgenic tobacco plants. Plant Mol. Biol. *55*, 61-81.

Lee, M.O., Hwang, J.H., Lee, D.H., and Hong, C.B. (2007). Gene expression profile for *Nicotiana tabacum* in the early phase of flooding stress. J. Plant Biol. *50*, 496-503.

Lee, H.K., Cho, S.K., Son, O., Xu, Z., Hwang, I., and Kim, W.T. (2009). Drought stress-induced Rma1H1, a RING membrane-anchor E3 ubiquitin ligase homolog, regulates aquaporin levels via ubiquitination in transgenic *Arabidopsis* plants. Plant Cell *21*, 622-641.

Neuwald, A.F., Aravind, L., Spouge, J.L., and Koonin, E.V. (1999). AAA+: a class of chaperone-like ATPases associated with the assembly, operation, and disassembly of protein complexes. Genome Res. *9*, 27-43.

Park, J.A., Cho, S.K., Kim, J.E., Chung, H.S., Hong, J.P., Hwang B., Hong, C.B., and Kim, W.T. (2003). Isolation of cDNAs differentially expressed in response to drought stress and characterization of the *Ca-LEAL1* gene encoding a new family of atypical LEA-LIKE protein homologue in hot pepper (*Capsicum annuum* L. cv. Pukang). Plant Sci. *165*, 471-481.

Park, J.-A., Kim, T.-W., Kim, S.-K., Kim, W.T., and Pai, H.-S. (2005a). Silencing of NbECR encoding a putative enoyl-CoA reductase results in disorganized membrane structure and epidermal cell ablation in *Nicotiana benthamiana*. FEBS Lett. *579*, 4459-4464.

Park, J.-A., Ahn, J.-W., Kim, Y.-K., Kim, S.J., Kim, J.-K., Kim, W.T., and Pai, H.-S. (2005b). Retinoblastoma protein regulates cell proliferation, differentiation, and endoreduplication in plants. Plant J. *42*, 153-163.

Park, S., Rancour, D.M., and Bednarek, S.Y. (2007). Protein domain-domain interactions and requirements for the negative regulation of *Arabidopsis* CDC48/p97 by the plant ubiquitin regulatory X (UBX) domain-containing protein, PUX1. J. Biol. Chem. *282*, 5217-5224.

Park, S., Rancour, D.M., and Bednarek, S.Y. (2008). In planta analysis of the cell cycle-dependent localization of AtCDC48A and its critical roles in cell division, expansion and differentiation. Plant Physiol. *148*, 246-258.

Partridge, J.J., Lopreiato, J.O., Latterich, M., and Indig, F.E. (2003). DNA damage modulates nucleolar interaction of the Werner protein with the AAA ATPase p97/VCP. Mol. Biol. Cell *14*, 4221-4229.

Rancour, D.M., Dickey, C.E., Park, S., and Bednarek, S.Y. (2002). Characterization of AtCDC48. Evidence for multiple membrane fusion mechanisms at the plane of cell division in plants. Plant Physiol. *130*, 1241-1253.

Rancour, D.M., Park, S., Knight, S.D., and Bednarek, S.Y. (2004). Plant UBX domain-containing protein 1, PUX1, regulates the oligomeric structure and activity of Arabidopsis CDC48. J. Biol. Chem. *279*, 54264-54274.

Ratcliff, F., Martin-Hernandez, A.M., and Baulcombe, D.C. (2001). Tobacco rattle virus as a vector for analysis of gene function by silencing. Plant J. *25*, 237-245.

Richly, H., Rape, M., Braun, S., Rumpf, S., Hoege, C., and Jentsch, S. (2005). A series of ubiquitin binding factors connects CDC48/p97 to substrate multiubiquitination and proteasomal targeting. Cell *120*, 73-84.

Rienties, I.M., Vink, J., Borst, J.W., Russinova, E., and de Vries, S.C. (2005). The *Arabidopsis* SERK1 protein interacts with the AAA-ATPase AtCDC48, the 14-3-3 protein GF14λ and the PP2C phosphatase KAPP. Planta *221*, 394-405.

Romisch, K. (2006). Cdc48 is UBX-linked to ER ubiquitin ligases. Trends Biochem. Sci. *31*, 24-25.

Sarowar, S., Lee, J.-Y., Ahn, E.-R., and Pai, H.-S. (2008). A role of hexokinases in plant resistance to oxidative stress and pathogen infection. J. Plant Biol. *51*, 341-346.

Seo, Y.S., Kim, E.Y., Mang, H.G., and Kim, W.T. (2008). Heterologous expression and biochemical and cellular characterization of *CaPLA1* encoding a hot pepper phospholipase A1 homolog. Plant J. *53*, 895-908.

Waterhouse, P.M., Wang, M.-B., and Lough, T. (2001). Gene silencing as an adaptive defense against viruses. Nature *411*, 834-842.

Yang, S.W., Kim, D.H., Lee J.J., Chun, Y.J., Lee, J.-H., Kim, Y.J., Chung, I.K., and Kim, W.T. (2003). Expression of the telomeric repeat binding factor gene *NgTRF1* is closely coordinated with the cell division program in tobacco BY-2 suspension culture cells. J. Biol. Chem. *278*, 21395-21407.

Yang, S.W., Kim, S.K., and Kim, W.T. (2004). Perturbation of *NgTRF1* expression induces apoptosis-like cell death in tobacco BY-2 cells and implicates NgTRF1 in the control of telomere length and stability. Plant Cell *16*, 3370-3385.

Ye, Y., Meyer, H.H., and Rapoport, T.A. (2001). The AAA ATPase Cdc48/p97 and its partners transport proteins from the ER into the cytosol. Nature *414*, 652-656.

Ye, Y., Meyer, H.H., and Rapoport, T.A. (2003). Function of the p97-Ufd1-Npl4 complex in retrotranslocation from the ER to the cytosol: dual recognition of nonubiquitinated polypeptide segments and polyubiquitin chains. J. Cell Biol. *162*, 71-84.

Yuan, X., Shaw, A., Zhang, X., Kondo, H., Lally, J., Freemont, P.S., and Matthews, S. (2001). Solution structure and interaction surface of the C-terminal domain from p47: a major p97-cofactor involved in SNARE disassembly. J. Mol. Biol. *311*, 255-263.